

# NUMERICAL APPROXIMATION OF THE INSITU COMBUSTION MODEL USING THE NONLINEAR MIXED COMPLEMENTARITY METHOD

JULIO CÉSAR AGUSTÍN SANGAY, ALEXIS RODRIGUEZ CARRANZA, GEORGE J. BAUTISTA,  
JUAN CARLOS PONTE BEJARANO, JOSÉ LUIS PONTE BEJARANO  
AND EDDY CRISTIAM MIRANDA RAMOS

**ABSTRACT.** In this work, we will study a numerical method that allows finding an approximation of the exact solution for a in-situ combustion model using the nonlinear mixed complementary method, which is a variation of the Newton's method for solving nonlinear systems based on an implicit finite difference scheme and a nonlinear algorithm mixed complementarity, FDA-MNCP. The method has the advantage of provide a global convergence in relation to the finite difference method and method of Newton that only has local convergence. The theory is applied to model in-situ combustion, which can be rewritten in the form of mixed complementarity also we do a comparison with the FDA-NCP method.

## CONTENTS

1. Introduction	1
2. Physical problem modeling	2
3. Description of the FDA-MNCP method for the simple in-situ combustion model	3
4. Comparison of FDA-MNCP and FDA-NCP methods	6
5. Error analysis	13
6. Conclusions	15
References	16

## 1. INTRODUCTION

several mathematical models in different disciplines such as engineering, physics, economics and other sciences study partial differential equations of the parabolic type. These models can lead to the problem of mixed complementarity, that is, the case several mathematical models in different disciplines, such as engineering, physics, economics and other sciences study partial differential equations of the parabolic type. These models can lead to the problem of mixed complementarity, that is, the case of the in-situ combustion model, which will be our model in this work. Other applications of complementarity problems are described in [9].

Since the goal is to find an approximation of the analytical solution, we will develop a numerical method that will allow us to achieve our goal. This technique will be applied to the simple in-situ combustion model which will be written as a mixed complementarity problem.

The in-situ combustion model is a particular case of the model treated in [4]. In this case, the model considers the injection of air into a porous medium containing solid fuel and consists of a system of two nonlinear parabolic differential equations.

The contribution of the work is the study of the simple in-situ combustion model and simulations for the proposed model applying the Crank-Nicolson method and the FDA-MNCP algorithm [6].

We will present the results that indicate that the sequence of feasible points generated is contained in a feasible region and we will verify that the directions obtained are feasible and descending for a function associated with the complementarity problem and we will also see the proof of global convergence for the FDA-MNCP following the feat for FDA-NCP[11]. We

apply the FDA-MNCP method to the in-situ combustion problem, describe the discretization procedure using the finite difference technique for the mixed complementarity problem associated with the problem, and also present the numerical results and the corresponding error analysis with the comparison with the FDA-NCP method. Finally, we will present some conclusions.

## 2. PHYSICAL PROBLEM MODELING

The model studies one-dimensional flows, with a combustion wave in the case when the oxidant (air with oxygen) is injected into a porous medium. Initially the medium contains a fuel that is essentially immobile, does not vaporize and the amount of oxygen is unlimited. This is the case for solid or liquid fuels with low saturations. As in [1], we study the simplified model where:

- A small part of the available space is occupied by fuel.
- Porosity changes in the reaction are negligible.
- Temperature of solid and gas are the same (local thermal equilibrium).
- Gas velocity is constant.
- Heat loss is negligible.
- Pressure variations are small compared to the prevailing pressure.

The model has temporal  $t$  and spatial  $x$  coordinates that include the heat balance equation, the molar balance equation for immobile fuels, and the ideal gas law.

$$C_m \frac{\partial T}{\partial t} + \frac{\partial}{\partial x}(C_g \rho u (T - T_{res})) = \lambda \frac{\partial^2 T}{\partial x^2} + Q_r W_r, \quad (1)$$

$$\frac{\partial \rho_f}{\partial t} = -\mu_f W_r, \quad (2)$$

$$\rho = \frac{P}{TR}, \quad (3)$$

where  $T[K]$  is the temperature,  $\rho[\frac{mol}{m^3}]$  is the molar density of the gas, and  $\rho_f[\frac{mol}{m^3}]$  is the molar concentration of the immobile fuel. The set of parameters along with their typical values are given in the Table1.

<i>Symbol</i>	<i>Physical Quantity</i>	<i>Value</i>	<i>Unit</i>
$T_{res}$	Initial reservoir temperature	273	[K]
$C_m$	Heat capacity of porous medium	$2 \cdot 10^6$	[J/m <sup>3</sup> K]
$c_g$	Heat capacity of gas	27.42	[J/molK]
$\lambda$	Thermal conductivity of porous medium	0.87	[J/(msK)]
$Q_r$	Enthalpy of the still fuel in $T_{res}$	$4 \cdot 10^5$	[J/mol]
$u_{inj}$	Darcy speed for gas injection (200m/dia)	0.0023	[m/s]
$E_r$	Activation energy	58000	[J/mol]
$K_p$	Pre-exponential parameter	500	1/s
$R$	Ideal gas constant	8.314	[J/molK]
$P$	Prevailing pressure (1atm)	101325	[Pa]
$\rho_f^{res}$	Initial molar density of fuel	372	[mol/m <sup>3</sup> ]

TABLE 1. Dimensional parameters for in-situ combustion and their typical values [1].

As in [1], if we consider for simplicity  $\mu_f = \mu_g = \mu_0 = 1$  and the amount of oxygen is unlimited, the reaction ratio  $W_r$  is taken as:

$$W_r = k_p \rho_f \exp\left(\frac{-E_r}{RT}\right). \quad (4)$$

The variables to be found are the temperature ( $T$ ) and the molar concentration of the immobile fuel ( $\rho_f$ ). Since the equations are not dimensioned, we do as [1], to obtain the dimensionless

form:

$$\frac{\partial \theta}{\partial t} + u \frac{\partial(\rho \theta)}{\partial x} = \frac{1}{P_{eT}} \frac{\partial^2 \theta}{\partial x^2} + \Phi(\theta, \eta). \quad (5)$$

$$\frac{\partial \eta}{\partial t} = \Phi(\theta, \eta). \quad (6)$$

$$\text{where: } \rho = \frac{\theta_0}{\theta + \theta_0}, \quad \Phi = \beta(1 - \eta) \exp\left(\frac{-E}{\theta + \theta_0}\right).$$

with the dimensionless constants:

$$P_{eT} = \frac{x^*}{\lambda \Delta T^*}, \quad \beta = \rho_f^* k_p Q_r, \quad E = \frac{E_r}{R \Delta T^*}, \quad \theta_0 = \frac{T_{res}}{\Delta T^*}, \quad u = \frac{u_{inj} t^*}{x^*}. \quad (7)$$

Here  $P_{eT}$  is the Peclet number for thermal diffusion,  $u$  becomes the dimensionless thermal wave velocity,  $E$  is a escalated activation energy and  $\theta_0$  is a scaled reservoir temperature. With a reservoir initial conditions:

$$t = 0; \quad x \geq 0 : \quad \theta = 0, \quad \eta = 0$$

and injections condition:

$$t \geq 0; \quad x = 0 : \quad \theta = 0, \quad \eta = 1.$$

### 3. DESCRIPTION OF THE FDA-MNCP METHOD FOR THE SIMPLE IN-SITU COMBUSTION MODEL

We now describe in detail the finite difference scheme for the in-situ combustion model for the FDA-MNCP method. For this we use the mesh applying the Crank-Nicolson method to approximate the spatial derivatives in each case, i.e.:

$$\partial_t \theta(x_m, t_{n+\frac{1}{2}}) = \frac{\theta_m^{n+1} - \theta_m^n}{k}. \quad (8)$$

$$\partial_{xx} \theta(x_m, t_{n+\frac{1}{2}}) = \frac{\theta_{m+1}^{n+1} - 2\theta_m^{n+1} + \theta_{m-1}^{n+1}}{2h^2} + \frac{\theta_{m+1}^n - 2\theta_m^n + \theta_{m-1}^n}{2h^2}. \quad (9)$$

$$\partial_x F(\theta(x_m, t_{n+\frac{1}{2}})) = \frac{F_{m+1}^{n+1} - F_{m-1}^{n+1}}{4h} + \frac{F_{m+1}^n - F_{m-1}^n}{4h}. \quad (10)$$

$$\Phi(\theta(x_m, t_{n+\frac{1}{2}})) = \frac{\Phi_m^{n+1} + \Phi_m^n}{2}. \quad (11)$$

Considering the Dirichlet conditions at the point  $x_0$ :

$$\theta(x_0, t) = 0, \quad \eta(x_0, t) = 1,$$

and Neumann conditions at the point  $x_M$

$$\frac{\partial \theta}{\partial x}(x_M, t) = 0, \quad \frac{\partial \eta}{\partial x}(x_M, t) = 0,$$

given in[20], therefore, the value at  $x_0$  is known at all times but not at  $x_M$ , and

$$\theta_0^{n+1} = \theta_0^n, \quad \eta_0^{n+1} = \eta_0^n, \quad \text{for all } n \in \mathbb{N} \quad (12)$$

The boundary condition on  $x_M$  gives:

$$\frac{\partial \theta}{\partial x}(x_M, t) = 0 \implies \frac{\theta_{M+1}^n - \theta_{M-1}^n}{2h} = 0$$

therefore,

$$\theta_{M+1}^n = \theta_{M-1}^n \implies F_{M+1}^n = F_{M-1}^n, \quad \text{for all } n \in \mathbb{N} \quad (13)$$

given shaping the FDA-MNCP method:

$$\theta \geq 0; \quad \frac{\partial \theta}{\partial t} + u \frac{\partial(\rho\theta)}{\partial x} - \frac{1}{P_{eT}} \frac{\partial^2 \theta}{\partial x^2} - \Phi(\theta, \eta) \geq 0. \quad (14)$$

$$\frac{\partial \eta}{\partial t} - \Phi(\theta, \eta) = 0. \quad (15)$$

To obtain the discrete relations of(14), we replace (8-11) in(14) to obtain:

$$\begin{aligned} -2\mu H\theta_{m-1}^{n+1} + (4 + 4\mu H)\theta_m^{n+1} - 2\mu H\theta_{m+1}^{n+1} + \lambda[F_{m+1}^{n+1} - F_{m-1}^{n+1}] - 2k\Phi_m^{n+1} &\geq \\ \geq 2\mu H\theta_{m-1}^n + (4 - 4\mu H)\theta_m^n + 2\mu H\theta_{m+1}^n + \lambda[F_{m+1}^n - F_{m-1}^n] + 2k\Phi_m^n, \end{aligned} \quad (16)$$

where  $\lambda = \frac{h}{h}$  and  $\mu = \frac{k}{hr}$ . The scheme is valid for  $m = 1, 2, \dots, M$  of the points whose values are not known. At the boundary points we have that for  $m = 1$ , substituting (12) in (16) we obtain:

$$\begin{aligned} (4 + 4\mu H)\theta_1^{n+1} - 2\mu H\theta_2^{n+1} + \lambda[F_2^{n+1} - F_0^{n+1}] - 2k\Phi_1^{n+1} &\geq \\ \geq (4 - 4\mu H)\theta_1^n + 2\mu H\theta_2^n - \lambda[F_2^n - F_0^n] + 2k\Phi_1^n + 4\mu H\theta_0^n, \end{aligned} \quad (17)$$

for  $n = M$ , we replace (13) in (16) for obtain:

$$-4\mu H\theta_{M-1}^{n+1} + (4 + 4\mu H)\theta_M^{n+1} - 2k\Phi_M^{n+1} \geq 4\mu H\theta_{M-1}^n + (4 - 4\mu H)\theta_M^n + 2k\Phi_M^n. \quad (18)$$

Then (16) is valid for all  $m = 2, \dots, M - 1$  and joining the expressions (17) and (18)we obtain the following inequality in the variable  $\theta^{n+1}$

$$G^n(\theta^{n+1}, \eta^{n+1}) = A\theta^{n+1} + \lambda P(\theta^{n+1}, \eta^{n+1}) - 2k\Phi(\theta^{n+1}, \eta^{n+1}) - LD(\theta^n, \eta^n) \geq 0, \quad (19)$$

where  $LD = B\theta^n - \lambda P(\theta^n, \eta^n) + 2k\Phi(\theta^n, \eta^n) + UR$  is known at every instant of time.

Furthermore:

$$A = \begin{bmatrix} 4 + 4\mu H & -2\mu H & 0 & 0 & \cdots & 0 & 0 & 0 \\ -2\mu H & 4 + 4\mu H & -2\mu H & 0 & \cdots & 0 & 0 & 0 \\ 0 & -2\mu H & 4 + 4\mu H & -2\mu H & & 0 & 0 & 0 \\ \vdots & & & & \ddots & & & \vdots \\ 0 & 0 & 0 & 0 & & -2\mu H & 4 + 4\mu H & -2\mu H \\ 0 & 0 & 0 & 0 & & 0 & -4\mu H & 4 + 4\mu H \end{bmatrix}, \quad (20)$$

$$B = \begin{bmatrix} 4 - 4\mu H & 2\mu H & 0 & 0 & \cdots & 0 & 0 & 0 \\ 2\mu H & 4 - 4\mu H & 2\mu H & 0 & \cdots & 0 & 0 & 0 \\ 0 & 2\mu H & 4 - 4\mu H & 2\mu H & & 0 & 0 & 0 \\ \vdots & & & & \ddots & & & \vdots \\ 0 & 0 & 0 & 0 & & 2\mu H & 4 - 4\mu H & 2\mu H \\ 0 & 0 & 0 & 0 & & 0 & 4\mu H & 4 - 4\mu H \end{bmatrix}, \quad (21)$$

$$P^n = P(\theta^n) = \begin{bmatrix} F_2^n - F_0^n \\ F_3^n - F_1^n \\ F_4^n - F_2^n \\ \vdots \\ F_M^n - F_{M-2}^n \\ 0 \end{bmatrix}, \quad \Phi^n = \Phi(\theta^n) = \begin{bmatrix} \Phi_1^n \\ \Phi_2^n \\ \Phi_3^n \\ \vdots \\ \Phi_{M-1}^n \\ \Phi_M^n \end{bmatrix}, \quad (22)$$

$$\theta^n = \begin{bmatrix} \theta_1^n \\ \theta_2^n \\ \theta_3^n \\ \vdots \\ \theta_{M-1}^n \\ \theta_M^n \end{bmatrix}, \quad UR = \begin{bmatrix} 4\mu H\theta_0^n \\ 0 \\ 0 \\ \vdots \\ 0 \\ 0 \end{bmatrix} \quad (23)$$

where  $A, B \in \mathbb{R}^{M \times M}$ ;  $\theta^n, P^n, \Phi^n \in \mathbb{R}^M$ . Similarly, to obtain the discrete form of (15) we replaced (8-11) in (15) to obtain:

$$Diag(2)\eta_m^{n+1} - k\Phi_m^{n+1} = Diag(2)\eta_m^n + k\Phi_m^n. \quad (24)$$

The difference scheme is valid for all  $m = 1, 2, \dots, M$  of the points whose values are not known.

At the boundary points we have that for  $m = 1$ , we replace (12) in (24) we obtain:

$$2\eta_1^{n+1} - k\Phi_1^{n+1} = 2\eta_1^n + k\Phi_1^n, \quad (25)$$

for  $m = M$ , we replaced (13) in (24) to obtain:

$$2\eta_M^{n+1} - k\Phi_M^{n+1} = 2\eta_M^n + k\Phi_M^n. \quad (26)$$

Therefore, (24) is valid for all  $m = 2, \dots, M-1$  and joining the expressions (25) and (26) we obtain the following inequality in the variable  $\eta^{n+1}$ ;

$$Q(\theta^{n+1}, \eta^{n+1}) = Diag(2)\eta^{n+1} - k\varphi(\theta^{n+1}, \eta^{n+1}) - LDQ(\theta^n, \eta^n), \quad (27)$$

where  $LDQ = Diag(2)\eta^n + k\varphi(\theta^n, \eta^n)$  is known at every instant of time.

Furthermore:

$$Diag(2) = \begin{bmatrix} 2 & 0 & 0 & 0 & \cdots & 0 & 0 & 0 \\ 0 & 2 & 0 & 0 & \cdots & 0 & 0 & 0 \\ 0 & 0 & 2 & 0 & & 0 & 0 & 0 \\ \vdots & & & & \ddots & & & \vdots \\ 0 & 0 & 0 & 0 & & 0 & 2 & 0 \\ 0 & 0 & 0 & 0 & & 0 & 0 & 2 \end{bmatrix}, \quad (28)$$

$$\varphi^n = \varphi(\theta, \eta^n) = \begin{bmatrix} \varphi_1^n \\ \varphi_2^n \\ \varphi_3^n \\ \vdots \\ \varphi_{M-1}^n \\ \varphi_M^n \end{bmatrix}, \quad \eta^n = \begin{bmatrix} \eta_1^n \\ \eta_2^n \\ \eta_3^n \\ \vdots \\ \eta_{M-1}^n \\ \eta_M^n \end{bmatrix}. \quad (29)$$

Therefore, the discrete form of (14) and (15) is given by (19) and (27).

$$G^n(\theta^{n+1}, \eta^{n+1}) \bullet \theta^{n+1} = 0, \quad (30)$$

$$Q^n(\theta^{n+1}, \eta^{n+1}) = 0, \quad (31)$$

and must comply with:

$$\theta^{n+1} \geq 0. \quad (32)$$

Thus, joining (19), (27) (30) and (32) form a Mixed Complementarity Problem, which can be solved by the FDA-MNCP algorithm

**Algoritmo 3.1** (implementation FDA-MNCP.).

**Step 1.** Do  $n = 0$  and  $N = 1/\Delta t$ .

**Step 2.** To obtain  $\theta^{n+1}$  and  $\eta^{n+1}$  we apply the method FDA – MNCP to solve the mixed complementarity problem.

$$\begin{aligned} G^n(\theta^{n+1}, \eta^{n+1}) \bullet \theta^{n+1} &= 0, \quad \theta^{n+1} \geq 0, \\ Q^n(\theta^{n+1}, \eta^{n+1}) &= 0 \end{aligned} \quad (33)$$

with

$$\begin{aligned} G^n(\theta^{n+1}, \eta^{n+1}) &= A\theta^{n+1} + \lambda P(\theta^{n+1}, \eta^{n+1}) - 2k\Phi(\theta^{n+1}, \eta^{n+1}) - LD(\theta^n, \eta^{n+1}) \geq 0, \\ Q(\theta^{n+1}, \eta^{n+1}) &= Diag(2) \cdot \eta^{n+1} - k\varphi(\theta^{n+1}, \eta^{n+1}) - LDQ(\theta^n, \eta^{n+1}) = 0. \end{aligned}$$

where the matrices  $A, B$  and the vectors  $P, \Phi$  and  $\varphi$  are given in (20), (21), (22), and (29).

**Step 3.** If  $n = N$  then **END**.

else  $n = n + 1$  return to Step 2

The numerical results obtained from the implementation of the Algorithm in Matlab are shown in the following Section.

#### 4. COMPARISON OF FDA-MNCP AND FDA-NCP METHODS

We will now present the numerical results of the simulations performed in Matlab for the FDA-MNCP method. For this simulation, we considered  $[x_0, x_M] = [0, 0.05]$  and  $[t_0, t_N] = [0, 1]$  as the space and time intervals respectively. We keep the numbers of subintervals in time constant and equal to:  $N = 10^5$ , that is,  $k = \Delta t = 10^{-5}$  while the number of subintervals in space will be equal to  $M = 50, 100, 200, 400$ . For the FDA-MNCP method we consider an error tolerance of  $10^{-8}$ .

The values of the dimensionless parameters in (7) are:

$$\begin{aligned} x^* &= 9,1 \times 10^4 [m], & t^* &= 1,48 \times 10^8 [s], & \Delta T^* &= 74,4 [K], \\ u^* &= 6,1 \times 10^{-4}, & P_{e_T} &= 1406, & \beta &= 7,44 \times 10^{10}, \\ E &= 93,8 & \theta_0 &= 3.67 & u &= 3,76. \end{aligned}$$

with the previous input data we obtain Figures (1), (2), (3), (4), which show the results obtained by algorithm 3.1 and algorithm 5 of [1] for the FDA-MNCP and FDA-NCP [11] methods, respectively.

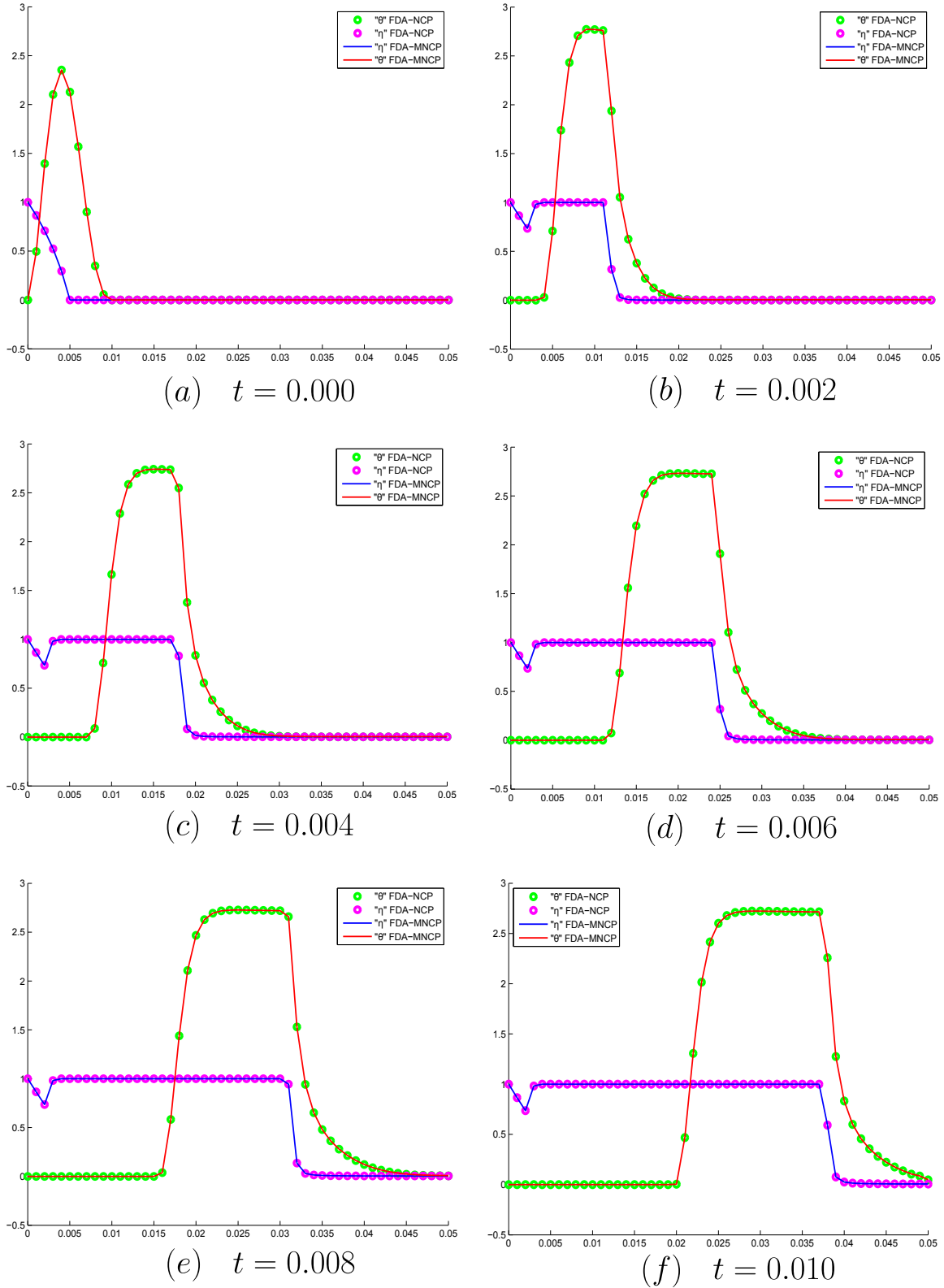


FIGURE 1. Comparison of the FDA-MNCP and FDA-NCP methods for  $M = 50$  at time instants  $t = 0.000, 0.002, 0.004, 0.006, 0.008, 0.010$ . The values of  $\theta$  are represented by green dots and a solid red line, the values of  $\eta$  are represented by pink dots and a solid blue line.

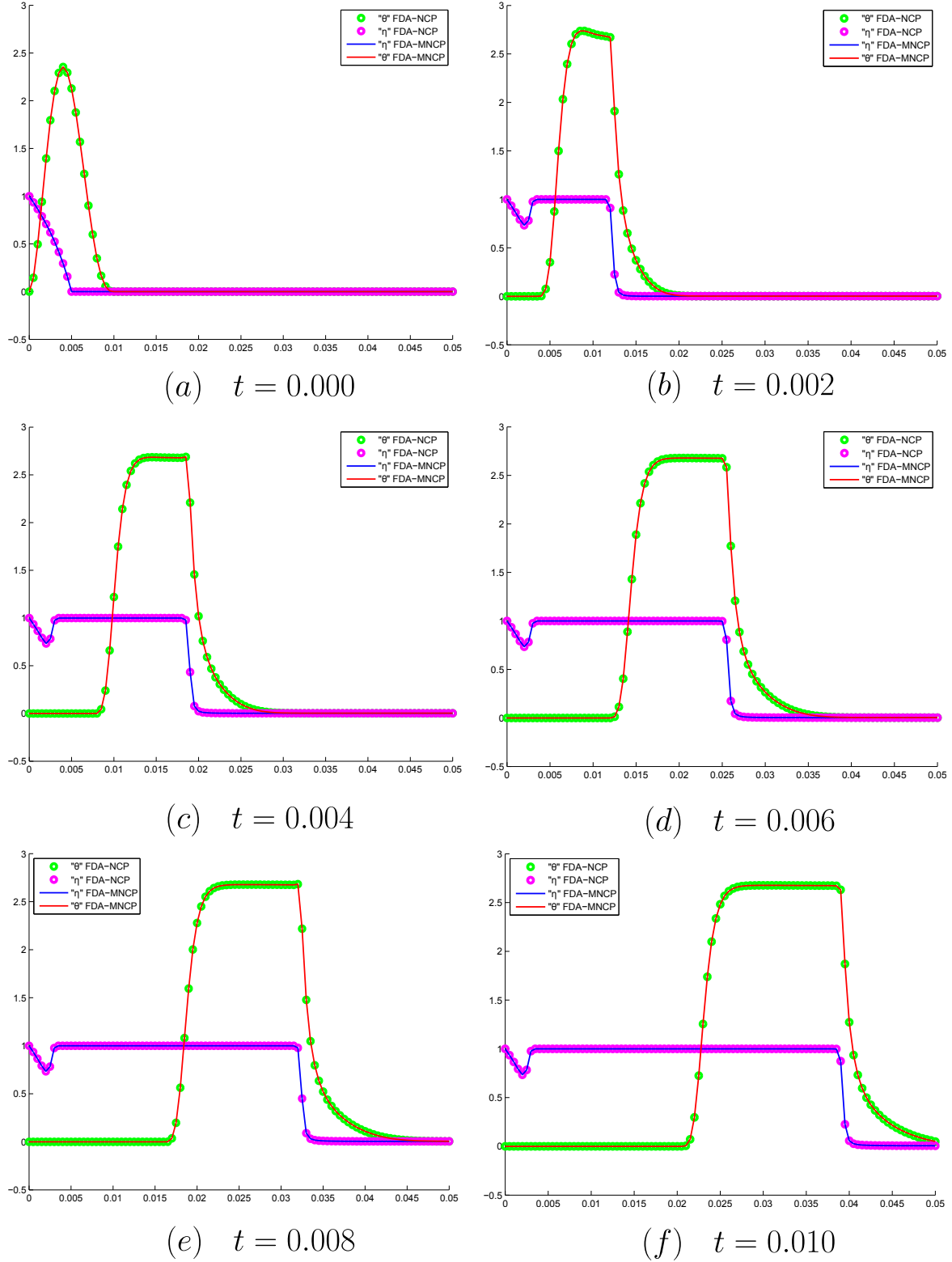


FIGURE 2. Comparison of the FDA-MNCP and FDA-NCP methods for  $M = 100$  at times  $t = 0.000, 0.002, 0.004, 0.006, 0.008, 0.010$ . The values of  $\theta$  are represented by green dots and a solid red line, the values of  $\eta$  are represented by pink dots and a solid blue line.



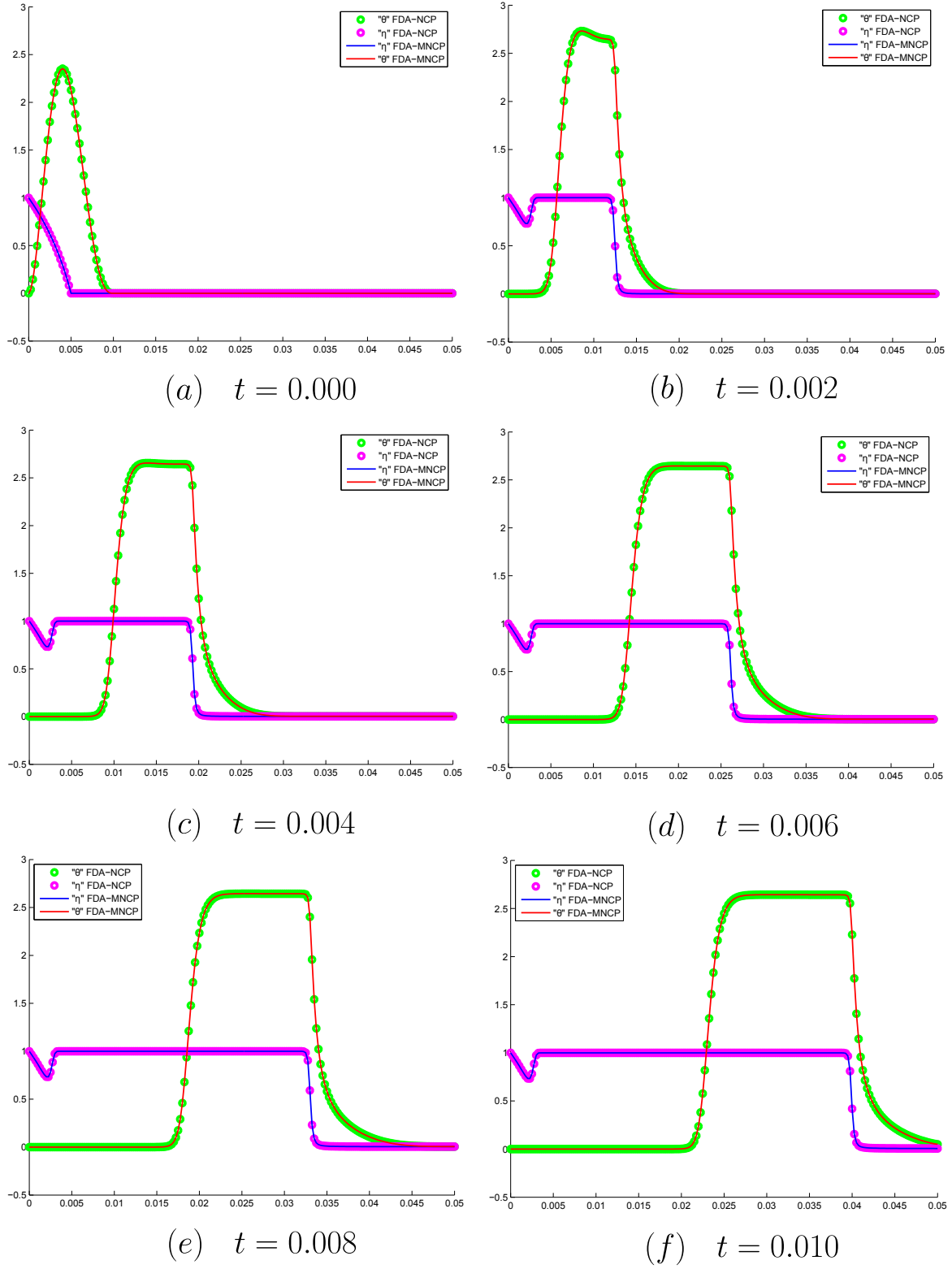


FIGURE 3. Comparison of the FDA-MNCP and FDA-NCP methods for  $M = 200$  at times  $t = 0.000, 0.002, 0.004, 0.006, 0.008, 0.010$ . The values of  $\theta$  are represented by green dots and a solid red line, the values of  $\eta$  are represented by pink dots and a solid blue line.

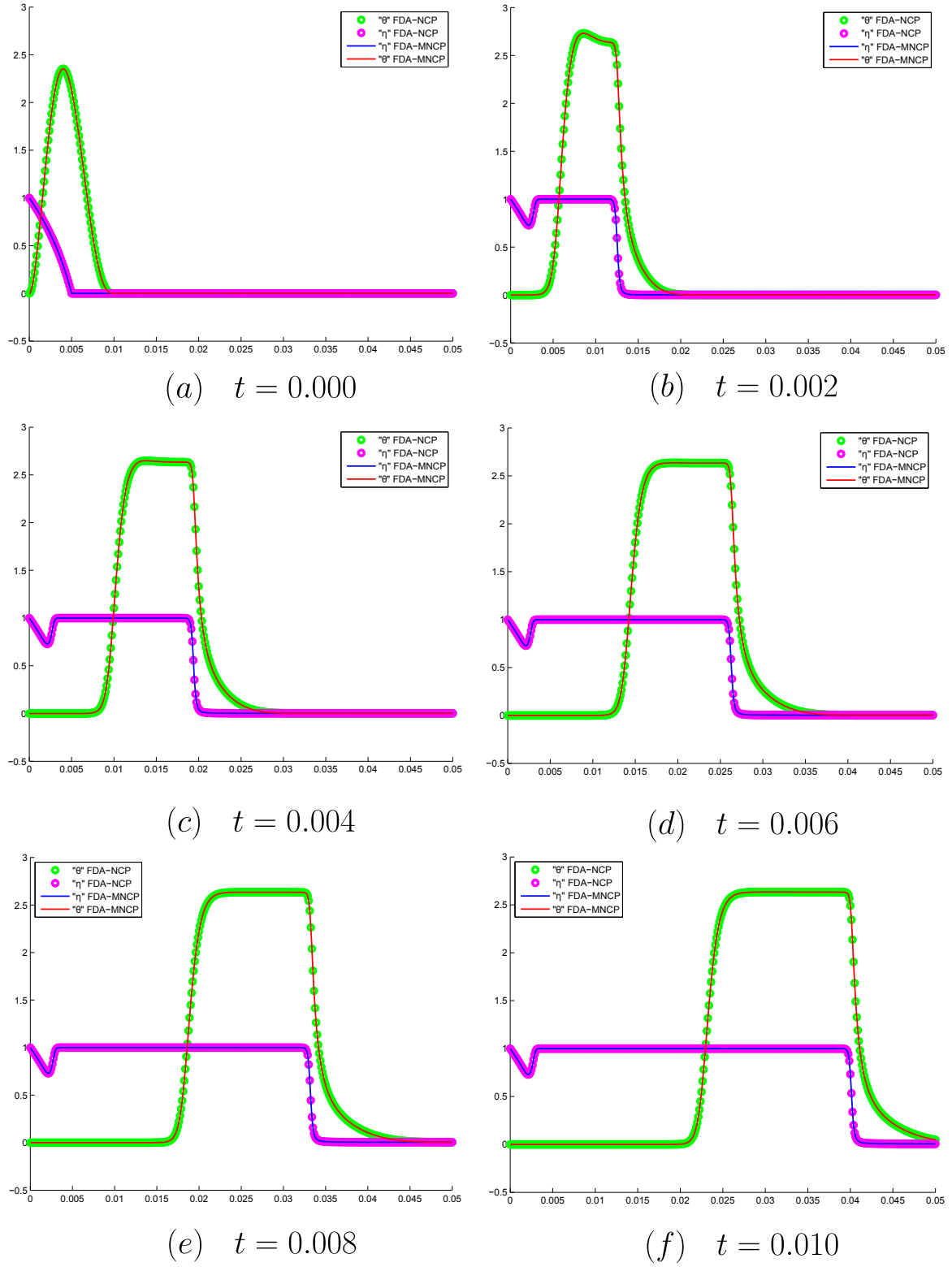


FIGURE 4. Comparison of the FDA-MNCP and FDA-NCP methods for  $M = 400$  at times  $t = 0.000, 0.002, 0.004, 0.006, 0.008, 0.010$ . The values of  $\theta$  are represented by green dots and a solid red line, the values of  $\eta$  are represented by pink dots and a solid blue line.

As we can see in Figures 1, 2, 3 and 4 obtained previously, they show us that the results obtained by the FDA-MNCP methods and FDA-NCP, coincide very well, as can be seen in the times indicated in the figures presented previously. In Figure 5, the differences between the methods can be observed.

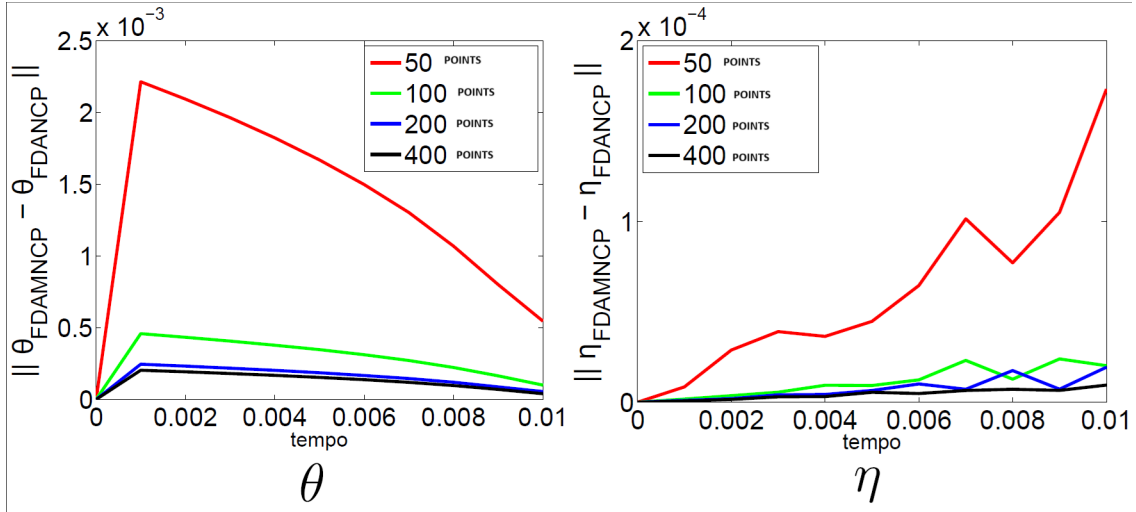


FIGURE 5. Difference between DA-NCP and FDA-NCP methods.

we can see that the difference between the solutions of  $\theta$  and  $\eta$  are very small as we increase the number of points, between the FDA-MNCP and FDA-NCP methods[11].

Below we show four tables where we compare the computational process time for  $M = 50, 100, 20, 400$  of the FDA-MNCP method and the FDA-NCP method studied in [1].

$t$	FDA-MNCP					FDA-NCP				
	$t(n)$	iter	BL(t)	$[S]$	$[\nabla S]$	$t(n)$	iter	BL(t)	$F$	$\nabla F$
0.001	0.401	33	1.0	43	34	0.194	20	1.0	43	40
0.002	0.411	34	0.8	44	35	0.194	20	1.0	43	40
0.003	0.406	34	1.0	43	35	0.199	20	1.0	43	40
0.004	0.386	32	0.8	41	33	0.184	20	1.0	43	40
0.005	0.385	32	0.8	41	33	0.178	21	1.0	45	42
0.006	0.406	34	0.8	43	35	0.198	21	1.0	45	42
0.007	0.395	33	0.8	42	34	0.193	21	1.0	45	42
0.008	0.403	33	0.8	43	34	0.229	21	1.0	45	42
0.009	0.390	32	0.8	42	33	0.169	21	1.0	45	42
0.010	0.405	33	0.8	44	34	0.173	21	1.0	45	42

TABLE 2. Comparison of the computational process time with  $M = 50$  for the FDA-MNCP and FDA-NCP methods.  $t(n)$  is the time measured in seconds that the method took to find the solution at time  $t$ .

As we can see in Table 2, the computational process time used by the FDA-MNCP method doubles the time of the FDA-NCP method for a partition of the  $x$ -axis into fifty points; the number of iterations of the FDA-MNCP method for the indicated times is also greater than that of the FDA-NCP method. In addition, the third column of each table shows the value of  $t^k$  for each of the methods.

$t$	FDA-MNCP					FDA-NCP				
	$t(n)$	iter	BL(t)	$[S]$	$[\nabla S]$	$t(n)$	iter	BL(t)	$F$	$\nabla F$
0.001	0.912	36	0.8	47	37	0.555	21	1.0	45	42
0.002	0.885	36	0.8	46	37	0.519	21	1.0	45	42
0.003	0.870	37	0.8	47	38	0.515	21	1.0	45	42
0.004	0.892	35	0.64	46	36	0.494	21	1.0	45	42
0.005	0.831	34	0.8	44	35	0.486	21	1.0	45	42
0.006	0.793	34	0.8	43	35	0.508	21	1.0	45	42
0.007	0.790	34	0.8	43	35	0.457	21	1.0	45	42
0.008	0.894	36	0.64	49	37	0.515	21	1.0	45	42
0.009	0.869	35	0.8	46	36	0.507	21	1.0	45	42
0.010	0.839	35	0.8	46	36	0.479	21	1.0	45	42

TABLE 3. Comparison of the computational process time with  $M = 100$  for the FDA-MNCP and FDA-NCP methods.  $t(n)$  is the time measured in seconds that the method took to find the solution at time  $t$ .

In Table 3, we can also observe that the computational process time used by the FDA-MNCP method is slightly greater than the time of the FDA-NCP method as the number of iterations.

$t$	FDA-MNCP					FDA-NCP				
	$t(n)$	iter	BL(t)	$[S]$	$[\nabla S]$	$t(n)$	iter	BL(t)	$F$	$\nabla F$
0.001	1.771	36	0.8	47	37	3.223	21	1.0	45	42
0.002	1.852	38	0.8	48	39	3.185	21	1.0	45	42
0.003	1.969	37	0.8	46	38	3.129	21	1.0	45	42
0.004	1.995	38	0.8	47	39	3.245	21	1.0	45	42
0.005	1.771	37	0.8	46	38	3.143	21	1.0	45	42
0.006	1.785	37	1.0	45	38	3.122	21	1.0	45	42
0.007	1.787	37	0.8	47	38	3.205	21	1.0	45	42
0.008	1.778	37	0.8	47	38	3.241	21	1.0	45	42
0.009	2.001	36	0.8	46	37	3.346	22	1.0	47	44
0.010	1.685	35	0.8	45	36	3.396	22	1.0	47	44

TABLE 4. Comparison of the computational process time with  $M = 200$  for the FDA-MNCP and FDA-NCP methods.  $t(n)$  is the time measured in seconds that the method took to find the solution at time  $t$ .

In Table 4, we see that when we increase the number of partitions to 200, the computational process time of the FDA-MNCP method starts to be shorter than the time of the 1FDA-NCP method, although the number of iterations is still greater.

$t$	FDA-MNCP					FDA-NCP				
	$t(n)$	iter	BL(t)	$[S]$	$[\nabla S]$	$t(n)$	iter	BL(t)	$F$	$\nabla F$
0.001	4.497	37	0.8	48	38	33.127	21	1.0	45	21
0.002	4.337	37	1.0	46	38	33.174	21	1.0	45	21
0.003	4.533	38	0.8	47	39	33.034	21	1.0	45	21
0.004	4.494	39	0.8	48	40	33.398	21	1.0	45	21
0.005	4.429	37	1.0	45	38	34.722	22	1.0	47	22
0.006	4.329	37	1.0	45	38	34.652	22	1.0	47	22
0.007	4.523	39	0.8	49	40	34.777	22	1.0	47	22
0.008	4.530	39	0.8	49	40	34.802	22	1.0	47	22
0.009	4.459	37	0.8	47	38	34.824	22	1.0	47	22
0.010	4.315	37	1.0	48	38	34.571	22	1.0	47	22

TABLE 5. Comparison of the computational process time with  $M = 400$  for the FDA-MNCP and FDA-NCP methods.  $t(n)$  is the time measured in seconds that the method took to find the solution at time  $t$ .

With the last Table 5, we can observe that by considerably increasing the number of partitions, the computational process time of the FDA-MNCP method is much lower than that of the FDA-NCP[11] method, because for the calculation of  $\nabla S$  in the FDA-MNCP method, it makes half the calculations than for  $\nabla F$  in the FDA-NCP[11] method, although the number of iterations is greater. We can also observe that the number of iterations varies little in each of the tables presented previously.

## 5. ERROR ANALYSIS

In this section we will perform a numerical study of the relative error for the FDA-MNCP method, for each instant of time and  $E_{\Delta x}$ , where  $\Delta x = h, h/2, h/4$ . The length of the subinterval in time will be constant and equal to  $\Delta t = k = 10^{-5}$  e  $h = \frac{1}{50}$ , and compared with the FDA-NCP method, [1]. Tables 6 and 8 show the results for the Relative Errors of the FDA-MNCP method, while Tables 7 and 9 show the Relative Error for the FDA-NCP method and are represented in Figures 6 and 7.

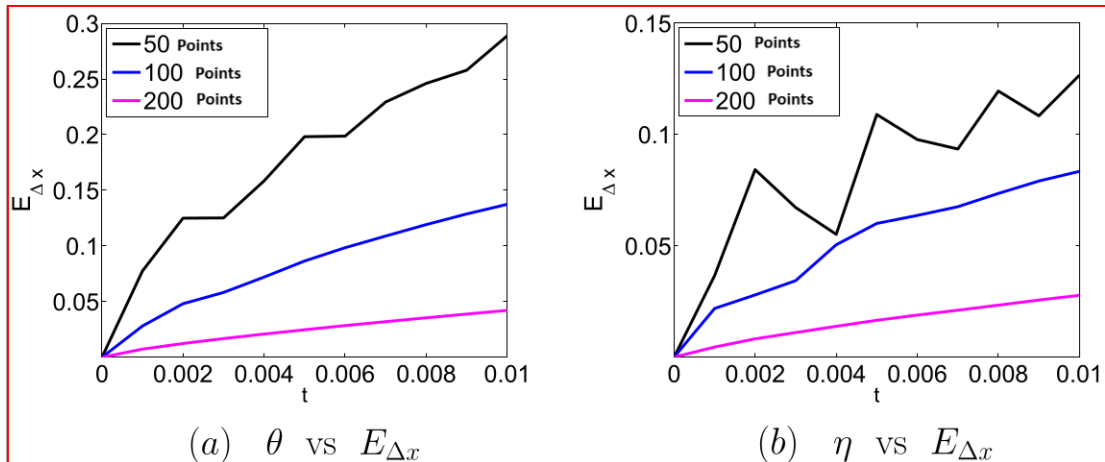


FIGURE 6. Time ( $t$ ) vs  $E_{\Delta x}$ . Relative Method Error. Here  $\Delta x = \frac{1}{50}, \frac{1}{100}, \frac{1}{200}$ .

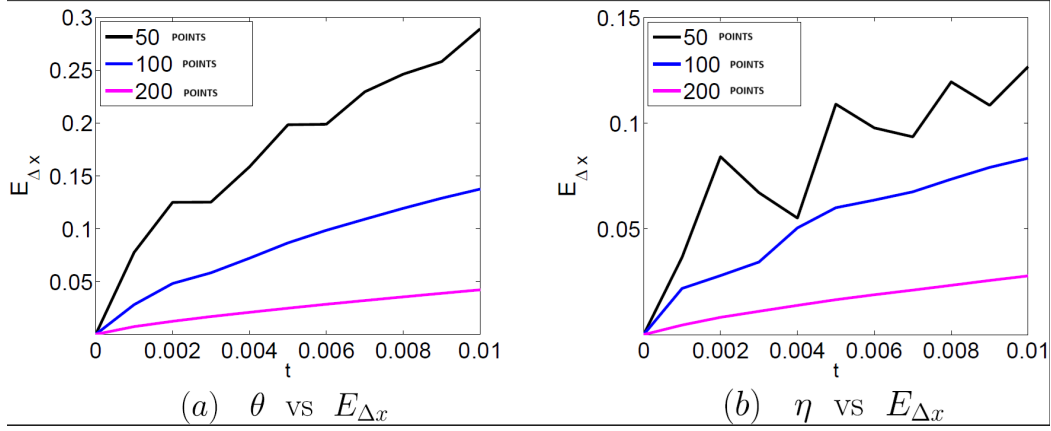


FIGURE 7. Time ( $t$ ) vs  $E_{\Delta x}$ . Relative Method Error FDA-NCP. Here  $\Delta x = \frac{1}{50}, \frac{1}{100}, \frac{1}{200}$ .

As can be seen in Figures 6 and 7, the relative errors corresponding to the FDA-MNCP and FDA-NCP methods, respectively, are very similar, as can be seen in the following tables, which show the relative errors for  $\theta$  and  $\eta$  usando  $h = 1/50$ .

$t$	$E_h$	$E_{\frac{h}{2}}$	$E_{\frac{h}{4}}$	$\frac{E_h}{E_{\frac{h}{2}}}$	$\frac{E_{\frac{h}{2}}}{E_{\frac{h}{4}}}$
0.00100000	0.07757130	0.02809022	0.00730451	2.76	3.85
0.00200000	0.12495960	0.04805076	0.01233415	2.60	3.90
0.00300000	0.12512590	0.05824369	0.01679689	2.15	3.47
0.00400000	0.15843617	0.07200921	0.02080162	2.20	3.46
0.00500000	0.19817638	0.08645161	0.02467447	2.29	3.50
0.00600000	0.19866653	0.09841438	0.02840411	2.02	3.46
0.00700000	0.22936049	0.10892940	0.03195340	2.11	3.41
0.00800000	0.24606770	0.11916519	0.03538988	2.06	3.37
0.00900000	0.25789027	0.12872004	0.03877097	2.00	3.32
0.01000000	0.28886846	0.13735367	0.04209700	2.10	3.26

TABLE 6. Relative error for  $\theta$  com FDA-MNCP e  $h = \frac{1}{50}$  for the time instants  $t$  indicated in the first column.

$t$	$E_h$	$E_{\frac{h}{2}}$	$E_{\frac{h}{4}}$	$\frac{E_h}{E_{\frac{h}{2}}}$	$\frac{E_{\frac{h}{2}}}{E_{\frac{h}{4}}}$
0.001	0.07753953	0.02808885	0.00730328	2.76	3.85
0.002	0.12490382	0.04804832	0.01233527	2.60	3.89
0.003	0.12507648	0.05824052	0.01679940	2.15	3.47
0.004	0.15841526	0.07200834	0.02080540	2.20	3.46
0.005	0.19818512	0.08645353	0.02467944	2.29	3.50
0.006	0.19869586	0.09841770	0.02841001	2.02	3.46
0.007	0.22940100	0.10893437	0.03196011	2.10	3.41
0.008	0.24613384	0.11917200	0.03539747	2.07	3.37
0.009	0.25797041	0.12872819	0.03877948	2.00	3.32
0.010	0.28897837	0.13736335	0.04210642	2.10	3.26

TABLE 7. Relative error for  $\theta$  com FDA-NCP e  $h = \frac{1}{50}$  for the time instants  $t$  indicated in the first column.

In Tables 6 and 7 we see that the relative errors  $E_h$ ,  $E_{\frac{h}{2}}$ ,  $E_{\frac{h}{4}}$  for  $\theta$  of both the FDA-MNCP method and the FDA-NCP method are very similar since they are the same in the first three decimal places.

$t$	$E_h$	$E_{\frac{h}{2}}$	$E_{\frac{h}{4}}$	$\frac{E_h}{E_{\frac{h}{2}}}$	$\frac{E_{\frac{h}{2}}}{E_{\frac{h}{4}}}$
0.00100000	0.03656879	0.02183277	0.00451877	1.67	4.83
0.00200000	0.08417410	0.02792488	0.00819559	3.01	3.41
0.00300000	0.06717364	0.03432880	0.01103677	1.96	3.11
0.00400000	0.05513563	0.05046208	0.01381861	1.09	3.65
0.00500000	0.10897196	0.06002542	0.01653614	1.82	3.63
0.00600000	0.09771893	0.06361601	0.01887177	1.54	3.37
0.00700000	0.09347666	0.06753455	0.02105732	1.38	3.21
0.00800000	0.11948456	0.07350345	0.02332175	1.63	3.15
0.00900000	0.10838295	0.07908666	0.02560247	1.37	3.09
0.01000000	0.12663557	0.08343716	0.02775604	1.52	3.01

TABLE 8. Relative error for  $\eta$  with FDA-MNCP and  $h = \frac{1}{50}$  for the instants of time  $t$  indicated in the first column.

$t$	$E_h$	$E_{\frac{h}{2}}$	$E_{\frac{h}{4}}$	$\frac{E_h}{E_{\frac{h}{2}}}$	$\frac{E_{\frac{h}{2}}}{E_{\frac{h}{4}}}$
0.001	0.03656752	0.02183277	0.00451876	1.67	4.83
0.002	0.08415103	0.02792385	0.00819578	3.01	3.41
0.003	0.06714517	0.03432836	0.01103751	1.96	3.11
0.004	0.05513010	0.05046448	0.01382034	1.09	3.65
0.005	0.10898570	0.06002658	0.01653867	1.82	3.63
0.006	0.09776211	0.06361489	0.01887480	1.54	3.37
0.007	0.09351854	0.06753575	0.02106120	1.38	3.21
0.008	0.11952653	0.07350797	0.02332674	1.63	3.15
0.009	0.10846255	0.07909222	0.02560830	1.37	3.09
0.010	0.12671978	0.08344353	0.02776237	1.52	3.01

TABLE 9. Relative error for  $\eta$  with FDA-NCP and  $h = \frac{1}{50}$  for the instants of time  $t$  indicated in the first column.

Similarly, in Tables 8 and 9 we  $E_h$ ,  $E_{\frac{h}{2}}$ ,  $E_{\frac{h}{4}}$  for  $\eta$  of both the FDA-MNCP method and the FDA-NCP method are very similar, since the first three decimal places are the same

## 6. CONCLUSIONS

- We propose the solution of the simple in-situ combustion model using a numerical method based on an implicit finite difference scheme and a nonlinear mixed complementarity algorithm, which can be applied to parabolic problems and can be rewritten in the form of a mixed complementarity problem. This method is applied to the system(1).
- In this work, we have seen that the feasible interior point algorithm FDA-MNCP, as a good technique to numerically solve mixed complementarity problems. Theoretical results of the algorithm ensure the global convergence.
- We solve the in-situ combustion model(1) using the nonlinear mixed complementarity algorithm and comparing it to the FDA-NCP method, with the two solutions being very close, as can be seen in Figures 1, 2, 3 and 4. This suggests that it is possible to apply this method to parabolic and hyperbolic problems, which can be written as a mixed complementarity problem. The FDA-MNCP method shows the advantage of being able

to be used with more points in the discretization of the space, as can be seen in Tables 4 and 5, in addition to being faster in computational time than the FDA-NCP method when we increase the discretization in the space.

- Regarding the relative errors, Tables 6 and 8 show good evidence of convergence of the mixed complementarity algorithm, which is observed in Figure 5, which indicates a decrease in linear growth when we refine the mesh.

## REFERENCES

- [1] RAMIREZ GUTIERREZ, ANGEL *Application of the nonlinear complementarity method for the study of in situ oxygen combustion* (Master's Thesis in Mathematics). Universidade Federal de Juiz de Fora, Juiz de Fora, Brasil, 2013.
- [2] BRUINING J., MARCHESIN D., and VAN DUIJN C.J. *Steam injection into water-saturated porous rock*. Computational e Applied Mathematics, 22(3):359-395, 2003.
- [3] BURDEN, R. L.; FAIRES, J. D. *Numerical Analysis*. Ninth edition. Boston, USA: Brooks/Cole - CENGAGE Learning, 2010.
- [4] CHAPIRO, G. ; MAZORCHE, S. R. ; HERSKOVITS, J. ; ROCHE, J. R. . *Solution of the Non-linear Parabolic Problems using Nonlinear Complementarity Algorithm (FDA-NCP)*. Mecánica Computacional, v. XXIX, p. 2141-2153, 2010.
- [5] DAKE L.P. *Fundamentals of reservoir engineering*. Elsevier, 1983.
- [6] DENNIS JR J.E. and SCHNABEL R.B. *Numerical Methods for Unconstrained Optimization and Nonlinear Equations*. Prentice-Hall, 1983.
- [7] DUIJN, C. J. V. *An Introduction to Conservation Laws: Theory and Applications to Multi-Phase Flow*. Eindhoven University of Technology, The Netherlands, 2003.
- [8] EL-BAKRY A.S. ,TAPIA R.A. , Y. ZHANG, and T. TSUCHIYA. *On the formulation and theory of the newton interior-point method for nonlinear programming*. Journal of Optimization Theory and Applications, 89(3):507-541, 1996.
- [9] FERRIS, M. C.; PANG, J. S. *Engineering and economic applications of complementarity problems*. Society for Industrial and Applied Mathematics, SIAM, v. 39, n. 4, 1997.
- [10] HERSKOVITS J., LEONTIEV A., DIAS G. and SANTOS G. *Contact Shape Optimization: A Bilevel Programming Approach*, Structural and Multidisciplinary Optimization 20, pp. 214-221.
- [11] HERSKOVITS J., MAZORCHE S. *A feasible directions algorithm for nonlinear complementarity problems and applications in mechanics*, Structural and Multidisciplinary Optimization, Feb 2009, vol 37, pp. 435-446.
- [12] LAWRENCE C. E. *Partial Differential Equations*. American Mathematical Society, 1997.
- [13] LEONTIEV A., HUACASI W. and HERSKOVITS J. *An Optimization Technique For The Solution Of The Signorini Problem Using The Boundary Element Method*, Structural and Multidisciplinary Optimization., 24, pp. 72-77.
- [14] LEVEQUE, R. J. *Numerical methods for conservation laws*. Lectures in mathematics: ETH Zurich, 1992.
- [15] MAYERS, D.; MORTON, K. *Numerical Solution of Partial Differential Equations*. Cambridge, UK.: Cambridge University Press, 2005.
- [16] OLEINIK, O. *Discontinuous Solutions of Nonlinear Differential Equations*. Amer. Math. Soc. Trans. Ser. 2, vol. 26, pp. 95-172, 1957.
- [17] SERRE, D. *Systems of Conservation Laws 1. Hyperbolicity, Entropies, Shock Waves*. Cambridge University Press, 1999.
- [18] SMOLLER, J. *Shock Waves and Reaction-Diffusion Equations*. 2da. ed. Springer Verlag, p.327, 1994.
- [19] STRIKWERDA, J. C. *Finite Difference Schemes and Partial Differential Equations*. Philadelphia, EE. UU.: Society for Industrial and Applied Mathematics, SIAM., 2004.
- [20] TANNEHILL, J. C.; ANDERSON, D. A.; PLETCHER, R. H. *Computational Fluid Mechanics and Heat Transfer*. W. J. Minkowycz and E. M. Sparrow, Editors, 1997.
- [21] THOMAS, J. *Numerical Partial Differential Equations. Conservation Laws and Elliptic Equations*. Springer-Verlag New York, Inc., 1999.



NUMERICAL APPROXIMATION OF THE INSITU COMBUSTION MODEL USING THE NONLINEAR MIXED COMPLEMENTARITY

J. SANGAY. UNIVERSIDAD PRIVADA DEL NORTE, TRUJILLO-PERÚ

*Email address:* julio.agustin@upn.edu.pe

A. RODRIGUEZ. UNIVERSIDAD PRIVADA DEL NORTE, TRUJILLO-PERÚ

*Email address:* alexis.rodriguez@upn.edu.pe

FACULTY OF ENGINEERING, CIVIL ENGINEERING PROFESSIONAL SCHOOL, TECHNOLOGICAL UNIVERSITY OF THE ANDES(UTEA), SEDE ABANCAY, AV. PERÚ 700, APURÍMAC, PERU.

*Email address:* gbautistas@utea.edu.pe

UNIVERSIDAD TECNOLÓGICA DEL PERU, TRUJILLO-PERÚ

*Email address:* C25226@utp.edu.pe

J. PONTE UNIVERSIDAD TECNOLÓGICA DEL PERU, TRUJILLO-PERÚ

*Email address:* c24064@utp.edu.pe

E. CRISTIAM UNIVERSIDAD NACIONAL DE TRUJILLO

*Email address:* emirandar@unitru.edu.pe